Suplemento de la Revista Mexicana de Física **3** 0308013 (2022) 1–4

Meson spectroscopy results from CMS

L. Lunerti for the CMS Collaboration

Dipartimento di Fisica e Astronomia, Università di Bologna, Viale Berti Pichat 6/2, Bologna, Italy.

Received 22 December 2021; accepted 24 February 2022

Recent results in meson spectroscopy with the CMS detector are presented. In particular, the first observation by the CMS Collaboration of two excited B_c^+ states and the measurement of the $B_c^+(2S)$ mass using proton-proton collisions at a center-of-mass energy of $13\,\mathrm{TeV}$ are reported.

Keywords: Meson; spectroscopy; CMS.

DOI: https://doi.org/10.31349/SuplRevMexFis.3.0308013

1. Introduction

The B_c^+ meson is the lightest meson composed of a bottom (b) and a charm (c) quark. Although observations and measurements of excited $\mathrm{b\bar{c}}$ states are scarce, the B_c^+ spectrum is predicted to be very populated. Since the $\mathrm{b\bar{c}}$ meson production cross section is proportional to the fourth power of the strong coupling constant (two pairs of heavy quarks need to be produced in the same hard scattering event), the B_c^+ production yield is significantly smaller than that of $\mathrm{b\bar{b}}$ and $\mathrm{c\bar{c}}$ mesons. The $\mathrm{b\bar{c}}$ mesons cannot annihilate into gluons: only decays through cascade emission of photons or pion pairs are expected for the excited states.

The B_c^+ and B_c^{*+} mass difference is predicted to be about $55\,\mathrm{MeV}$, while $B_c^+(2S)$ and $B_c^{*+}(2S)$ masses differ by around $35\,\mathrm{MeV}$ [1-3]. The $B_c^+(2S)$ state decays directly to $B_c^+\pi^+\pi^-$ while the $B_c^{*+}(2S)$ state decays to $B_c^{*+}\pi^+\pi^-$ followed by the $B_c^{*+} \to B_c^+\gamma$ decay. The energy of the photon is expected to be very low and it stays undetected. For this reason, the $B_c^{*+}(2S)$ mass peak in the $B_c^+\pi^+\pi^-$ invariant mass spectrum is expected to be shifted by ΔM with respect to the $B_c^+(2S)$ mass, where $\Delta M \equiv [M(B_c^{*+}) - M(B_c^+)] - [M(B_c^{*+}(2S)) - M(B_c^+(2S))]$. The $B_c^+(2S)$ and $B_c^{*+}(2S)$ states can be observed as two separate peaks in the $B_c^+\pi^+\pi^-$ invariant mass distribution only if ΔM is larger than the experimental resolution. Since $M(B_c^{*+}) - M(B_c^+)$ is expected to be larger than $M(B_c^{*+}(2S)) - M(B_c^+(2S))$, the $B_c^{*+}(2S)$ mass peak will appear as the lower one. The B_c^+ candidate is reconstructed targeting its decay to $J/\psi\pi^+$, where $J/\psi \to \mu^+\mu^-$.

The CMS [4] Collaboration observed two well resolved signals consistent with the $B_c^+(2S)$ and $B_c^{*+}(2S)$ states using data recording proton-proton collisions at $\sqrt{s} = 13\,\mathrm{TeV}$ during the 2015-2018 period at the CERN LHC, and corresponding to a total integrated luminosity of $143\,\mathrm{fb}^{-1}$ [5] (reported in Sec. 2). In addition, a measurement of the $B_c^+(2S)$ to B_c^+, the $B_c^{*+}(2S)$ to B_c^+ and the $B_c^{*+}(2S)$ to $B_c^+(2S)$ cross section ratios, as well as a measurement of the dipion invariant mass distribution coming from the $B_c^{(*)+}(2S) \to B_c^{(*)+}\pi^+\pi^-$ have been performed [6] (reported in Sec. 3). Systematic uncertainties measurement is reported in Sec. 4.

2. Observation of $B_c^+(2S)$ and $B_c^{*+}(2S)$ states

The offline event selection is performed by requiring the presence of an oppositely charged muon pair matching the one that triggered the detector readout. The B_c^+ candidate is built by combining this muon pair with a track, assumed to be a pion. The B_c^+ candidate is then obtained by performing a kinematic fit on the selected dimuon pair and a pion track, requiring them to form a common vertex and constraining the dimuon mass to the world average J/ψ mass [7].

The following requirements are then applied to B_c^+ candidates: transverse momentum $p_T > 15\,\mathrm{GeV}$, rapidity $|y| < 2.4$, decay length $l > 100\,\mu\mathrm{m}$ and a kinematic fit χ^2 probability larger than 10%. If more than one B_c^+ candidate is found in the event, the one having the highest p_T is selected. The decay length is measured as the three-dimensional distance of the decay vertex to the primary vertex (PV). The PV is chosen among all reconstructed vertices as the one having the smallest angle between the B_c^+ candidate momentum and the vector pointing from the PV to the decay vertex.

In order to extract the B_c^+ signal peak, the $J/\psi\pi^+$ invariant mass distribution is fitted taking into account the following background sources: (i) combinatorial background modeled using a first order Chebyshev polynomial function; (ii) partially reconstructed $B_c^+ \to J/\psi\pi^+X$ decays described by a generalized ARGUS function [8] convolved with a Gaussian resolution function and (iii) a small contribution coming from $B_c^+ \to J/\psi K^+$ whose shape has been determined by means of simulated samples and the normalization has been fixed relative to $B_c^+ \to J/\psi\pi^+$ yield taking into account their branching fraction and reconstruction efficiency ratio. The fitted B_c^+ candidate invariant mass distribution is shown in Fig. 1.

The $B_c^+(2S)$ and $B_c^{*+}(2S)$ candidates are reconstructed by performing a kinematic fit of a B_c^+ candidate with a pair of oppositely charged tracks, assumed to be pions, and impos-

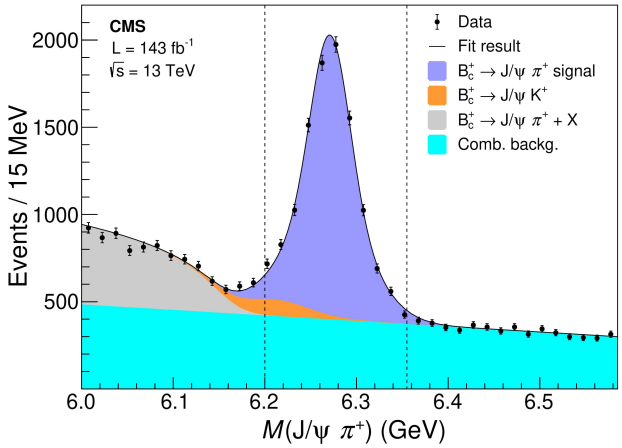

FIGURE 1. The invariant mass distribution of B_c^+ candidates. The vertical dashed lines indicate the mass window retained for the reconstruction of the $B_c^+(2S)$ and $B_c^{*+}(2S)$ candidates. The vertical bars on the points represent the statistical uncertainty in the data. The contributions from various sources are shown by the stacked distributions. The solid line represents the result of the fit. From Ref. [5].

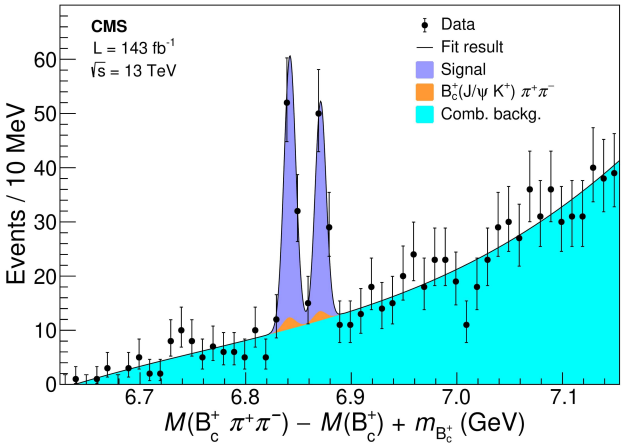

FIGURE 2. The $M(B_c^+\pi^+\pi^-) - M(B_c^+) + m_{B_c^+}$ distribution. The vertical bars on the points represent the statistical uncertainty in the data. The contributions from the various sources are shown by the stacked distributions. The solid line represents the result of the fit. From Ref. [5].

ing a common vertex. Only B_c^+ candidates having a mass between 6.2 and $6.355\,\mathrm{GeV}$ are taken into account. In addition, one of the pion cadidate is required to have $p_T > 0.8\,\mathrm{GeV}$ and the other $p_T > 0.6\,\mathrm{GeV}$. The $B_c^+\pi^+\pi^-$ candidate must have $|y| < 2.4$ and a vertex χ^2 probability larger than 10%. Event selection criteria have been optimized using $S/\sqrt{S+B}$ figure of merit, where signal (S) and background (B) events have been measured using simulated signal samples and sideband events, respectively.

Signal peaks belonging to $B_c^+(2S)$ and $B_c^{*+}(2S)$ candidate are inferred by fitting the $M(B_c^+\pi^+\pi^-) - M(B_c^+) + m_{B_c^+}$ distribution, where M indicates the invariant mass and $m_{B_c^+}$ is the world average B_c^+ mass [7]. This variable has been used in place of $M(B_c^+\pi^+\pi^-)$ because it has a better resolution. The two signal peaks have been modeled using a Breit-Wigner convolved with a Gaussian resolution function. Two main sources of background have been taken into account: combinatorial background, modeled using a third-order Chebyshev polinomial, and events coming from $B_c^+ \to J/\psi K^+$ candidates, fitted using the same shape as the signal peaks and normalized to the expected ratio of the $B_c^+ \to J/\psi K^+$ and $B_c^+ \to J/\psi\pi^+$ yields in the B_c^+ mass window and corrected by their corresponding reconstruction efficiency ratio.

The fitted $M(B_c^+\pi^+\pi^-) - M(B_c^+) + m_{B_c^+}$ distribution is shown in Fig. 2. The $B_c^+(2S)$ and $B_c^{*+}(2S)$ signal are well resolved with a mass difference of $\Delta M = 29.1 \pm 1.5\,(\mathrm{stat}) \pm 0.7\,(\mathrm{syst})\,\mathrm{MeV}$. The $B_c^+(2S)$ mass is measured to be $6871.0 \pm 1.2\,(\mathrm{stat}) \pm 0.8\,(\mathrm{syst}) \pm 0.8\,(B_c^+)\,\mathrm{MeV}$, where the last term refers to the uncertainty on the world-average B_c^+ mass. The observation of two peaks instead of one has been established with a significance of 6.5 standard deviations. These results have been confirmed by LHCb collaboration [9].

3. Cross section ratios and dipion invariant mass distribution measurements

The $B_c^+(2S)$ to B_c^+, the $B_c^{*+}(2S)$ to B_c^+ and the $B_c^{*+}(2S)$ to $B_c^+(2S)$ cross section ratios, denoted by R^+, R^{*+} and R^+/R^{*+}, have been determined by computing the ratio of the measured yields, corrected for the detection efficiency. Since the $J/\psi \to \mu^+\mu^-$ trigger efficiency affects both the B_c^+ and the $B_c^{(*)+}(2S)$ reconstruction, it cancels out when performing the cross section ratio.

The only efficiency that has to be taken into account is associated with the event reconstruction. All three reconstruction efficiencies have been measured by means of simulated samples. The number of B_c^+, $B_c^+(2S)$ and $B_c^{*+}(2S)$ mesons that survived downstream of the reconstruction chain divided by the number of mesons generated upstream of the Monte Carlo (MC) simulation chain is the reconstruction efficiency. The measured cross section ratios are: $R^+ = 3.47 \pm 0.63\,(\mathrm{stat}) \pm 0.33\,(\mathrm{syst})\%$, $R^{*+} = 4.69 \pm 0.71\,(\mathrm{stat}) \pm 0.56\,(\mathrm{syst})\%$ and $R^{*+}/R^+ = 1.35 \pm 0.32\,(\mathrm{stat}) \pm 0.09\,(\mathrm{syst})\%$.

The dependence of the cross section ratios on the transverse momentum p_T and the rapidity y of the B_c^+ meson has been tested. In Figs. 3 and 4, R^+ and R^{*+} ratios (upper panel) and R^{*+}/R^+ (lower panel) are displayed as a function of the B_c^+ candidate p_T and y, respectively. Statistical only uncertainties are showed. Reporting the cross section ratios as a function of B_c^+ kinematics allows to cancel to the large extent systematic uncertainties related to B_c^+ detection. Within the probed p_T and y regions, none of the measured cross section ratios show a clear dependence on these variables.

Figure 5 shows the normalized invariant mass distribution of the pion pair coming from $B_c^{*+}(2S)$ and $B_c^+(2S)$ compa-

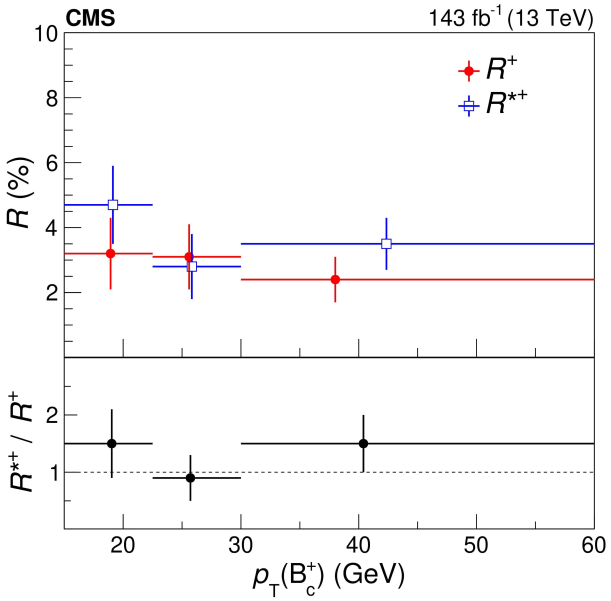

FIGURE 3. The R^+ and R^{*+} cross section ratios (upper panel) and R^{*+}/R^+ (lower panel), including $B_c^{(*)+}(2S) \rightarrow B_c^{(*)+}\pi^+\pi^-$ branching fraction, displayed as a function of B_c^+ candidate transverse momentum p_T. The markers are shown at the average B_c^+ p_T or $|y|$ values of the events contributing to each bin. Vertical bars represent statistical uncertainty only. From Ref. [6].

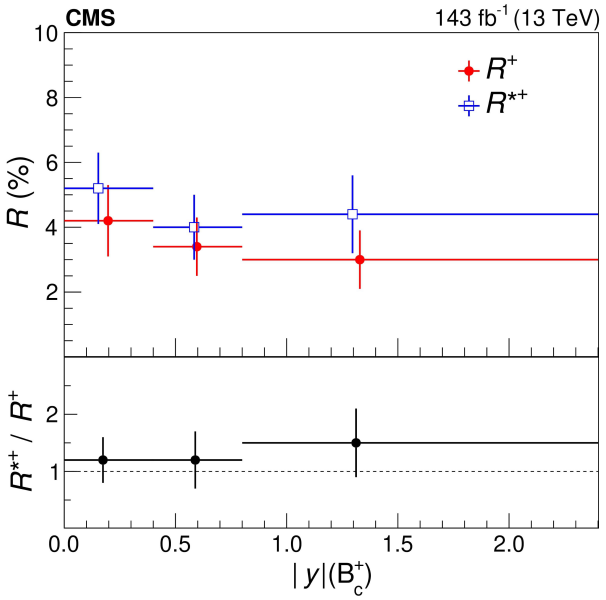

FIGURE 4. The R^+ and R^{*+} cross section ratios (upper panel) and R^{*+}/R^+ (lower panel), including $B_c^{(*)+}(2S) \rightarrow B_c^{(*)+}\pi^+\pi^-$ branching fraction, displayed as a function of B_c^+ candidate rapidity y. The markers are shown at the average B_c^+ p_T or $|y|$ values of the events contributing to each bin. Vertical bars represent statistical uncertainty only. From Ref. [6].

red with the expected distribution from MC, after background subtraction. The $B_c^{(*)+}(2S)$ dipion invariant mass distributions in data are compatible with each other while they show a different shape with respect to MC, which assumes no kine-

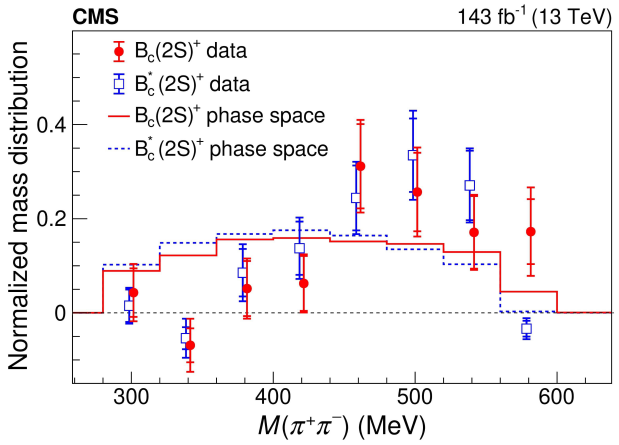

FIGURE 5. The $\pi^+\pi^-$ from $B_c^{(*)+}(2S)$ decay invariant mass distribution in data (blue and red marks) and in MC (continuous line). Error bars in data take into account statistical (inner mark) and systematic (outer mark) uncertainties. From Ref. [6].

matic correlation between pions. The dipion invariant mass in data suggests the presence of an intermediate resonance, which could be compatible with $f_0(500)$ mass.

4. Systematic uncertainties

For each of the sources of systematic uncertainty, the analysis has been repeated. Any variation with respect to the baseline analysis has been considered as systematic uncertainty.

Systematic uncertainties affecting the B_c^+ yield have been evaluated by independently varying the signal and background models used in the fit. The corresponding uncertainty for signal (background) is 4.3% (3.5%) and affects in the same way R^+ and R^{*+}, while it cancels out in R^{*+}/R^+. The $B_c^+(2S)$ and $B_c^{*+}(2S)$ yields are also affected by how signal and background are modeled. The systematic uncertainty on the signal modeling has been evaluated by fitting the background-only region of the spectrum and then subtracting the background yield to the signal region. The systematic uncertainty affecting the background has been measured by varying the fit function. The usage of alternative $B_c^+(2S)$ and $B_c^{*+}(2S)$ yields measurements leads to a systematic uncertainty of 5.9%, 2.9% and 2.9% for R^+, R^{*+} and R^{*+}/R^+, respectively.

Two sources of systematic uncertainties related to reconstruction efficiencies have been taken into account: potential residual mismatches between the running conditions and the settings used in simulations account for 1.8%, 1.6% and 0.9% for R^+, R^{*+} and R^{*+}/R^+, respectively; the uncertainty in the reconstruction efficiency of the two pions emitted in the $B_c^{(*)+}(2S) \rightarrow B_c^{(*)+}\pi^+\pi^-$ decay account for 4.2% for R^+ and R^{*+}, and it cancels out in R^{*+}/R^+. Systematic uncertainties on the reconstruction efficiency measurement are directly propagated into systematic uncertainties on the cross section ratios.

In the $B_c^{(*)+}(2S) \rightarrow B_c^{(*)+}\pi^+\pi^-$ decay, the two pions are considered to be kinematically unrelated. In order to take

into account that the pion pair kinematics (a) may depend upon the existence of an intermediate resonance or (b) may be affected by the different spins of $B_c^{*+}(2S)$ and $B_c^+(2S)$ mesons, the analysis has been repeated after re-weighting the MC samples to match the $\pi^+\pi^-$ invariant mass distribution ('decay kinematics') or the B_c^+-π angle in the dipion rest frame ('helicity angle'). Systematic uncertainties are counted as the differences between the resulting ratios of reconstruction efficiencies and those obtained in the baseline scenario: 1.5%, 6.9%, and 4.2% for the decay kinematics, and 1.0%, 6.0%, and 3.5% for the helicity angle, respectively, for R^+, R^{*+} and R^{*+}/R^+. The total systematic uncertainty is the sum in quadratures of the individual uncertainties.

5. Summary

Signals consistent with $B_c^+(2S)$ and $B_c^{*+}(2S)$ states have been observed for the first time by investigating the $B_c^{(*)+} \to B_c^{(*)+}\pi^+\pi^-$ decay channel, followed by $B_c^+ \to J\psi\pi$ and $J/\psi \to \mu^+\mu^-$ decays. The ΔM between $B_c^+(2S)$ and $B_c^{*+}(2S)$ peaks has been measured to be $29.1 \pm 1.5\,(\text{stat}) \pm 0.7\,(\text{syst})$ MeV, and the $B_c^+(2S)$ mass is measured to be $6871.0 \pm 1.2\,(\text{stat}) \pm 0.8\,(\text{syst}) \pm 0.8\,(B_c^+)$ MeV. In addition, a measurement of the $B_c^+(2S)$ to B_c^+, the $B_c^{*+}(2S)$ to B_c^+ and the $B_c^{*+}(2S)$ to $B_c^+(2S)$ cross section ratios, R^+, R^{*+} and R^{*+}/R^+ has been reported. The measured cross section ratios are:

$$R^+ = 3.47 \pm 0.63\,(\text{stat}) \pm 0.33\,(\text{syst})\%,$$

$$R^{*+} = 4.69 \pm 0.71\,(\text{stat}) \pm 0.56\,(\text{syst})\% \text{ and}$$

$$R^{*+}/R^+ = 1.35 \pm 0.32\,(\text{stat}) \pm 0.09\,(\text{syst})\%.$$

Furthermore, R^+, R^{*+} and R^{*+}/R^+ do not show any dependence on B_c^+ rapidity or transverse momentum.

A measurement of the dipion invariant mass distribution coming from the $B_c^{(*)+}(2S) \to B_c^{(*)+}\pi^+\pi^-$ has also been reported. The dipion invariant mass distribution in data is different than the one observed using simulated samples, that have been produced assuming no kinematic correlation between the two muons. This could suggest the presence of an intermediate resonance. All the reported measurements have been performed using data collected by CMS at a center-of-mass energy of 13 TeV.

These measurements make a significant contribution to the detailed characterization of heavy meson spectroscopy and allow to probe the nonperturbative QCD interactions that bind heavy quarks into hadrons.

1. E. B. Gregory *et al*., Prediction of the B_c^* mass in full lattice qcd. *Phys. Rev. Lett*., **104** (2010) 022001.
2. R. J. Dowdall, C. T. H. Davies, T. C. Hammant, and R. R. Horgan. Precise heavy-light meson masses and hyperfine splittings from lattice qcd including charm quarks in the sea. *Phys. Rev. D*, **86** (2012) 094510.
3. Nilmani Mathur, M. Padmanath, and Sourav Mondal. Precise predictions of charmed-bottom hadrons from lattice qcd. *Phys. Rev. Lett.*, **121** (2018) 202002.
4. CMS Collaboration. The CMS experiment at the CERN LHC. *Journal of Instrumentation*, **3** (2008) S08004.
5. CMS Collaboration. Observation of two excited B_c^+ states and measurement of the $B_c^+(2s)$ mass in pp collisions at $\sqrt{s} = 13$ TeV. *Phys. Rev. Lett*. **122** (2019) 132001.
6. CMS Collaboration. Measurement of $B_c(2S)^+$ and $B_c^*(2S)^+$ cross section ratios in proton-proton collisions at $\sqrt{s} = 13$ TeV. *Phys. Rev. D* **102** (2020) 092007.
7. Particle Data Group. Review of particle physics. *Phys. Rev. D*, **98** (2018) 030001.
8. ARGUS Collaboration. Search for hadronic bâu decays. *Physics Letters B*, **241** (1990) 278.
9. LHCb Collaboration. Observation of an excited B_c^+ state. *Phys. Rev. Lett*., **122** (2019) 232001.